ETH zürich

Enhanced photoelectrical performance of dye-sensitized solar cells (DSSCs) with novel electrodes

Shutao Wang

Contents

Contents

Background

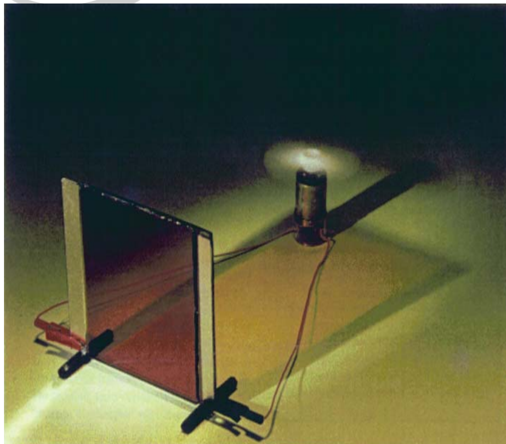

Developing clean energy alternatives to fossil fuels technology has become one of the most important tasks undertaken by modern science.

Alternative to silicon solar cell
——Grätzel

Solar cell

- **Crystalline Silicon**
- **Thin Film**
- **Organic/ Polymer**
- **DSSCs**

※ **Ref:** B. O'Regan, M. Grätzel, *Nature*, 1991, **353**, 737.

Conversion Efficiencies vs. Time

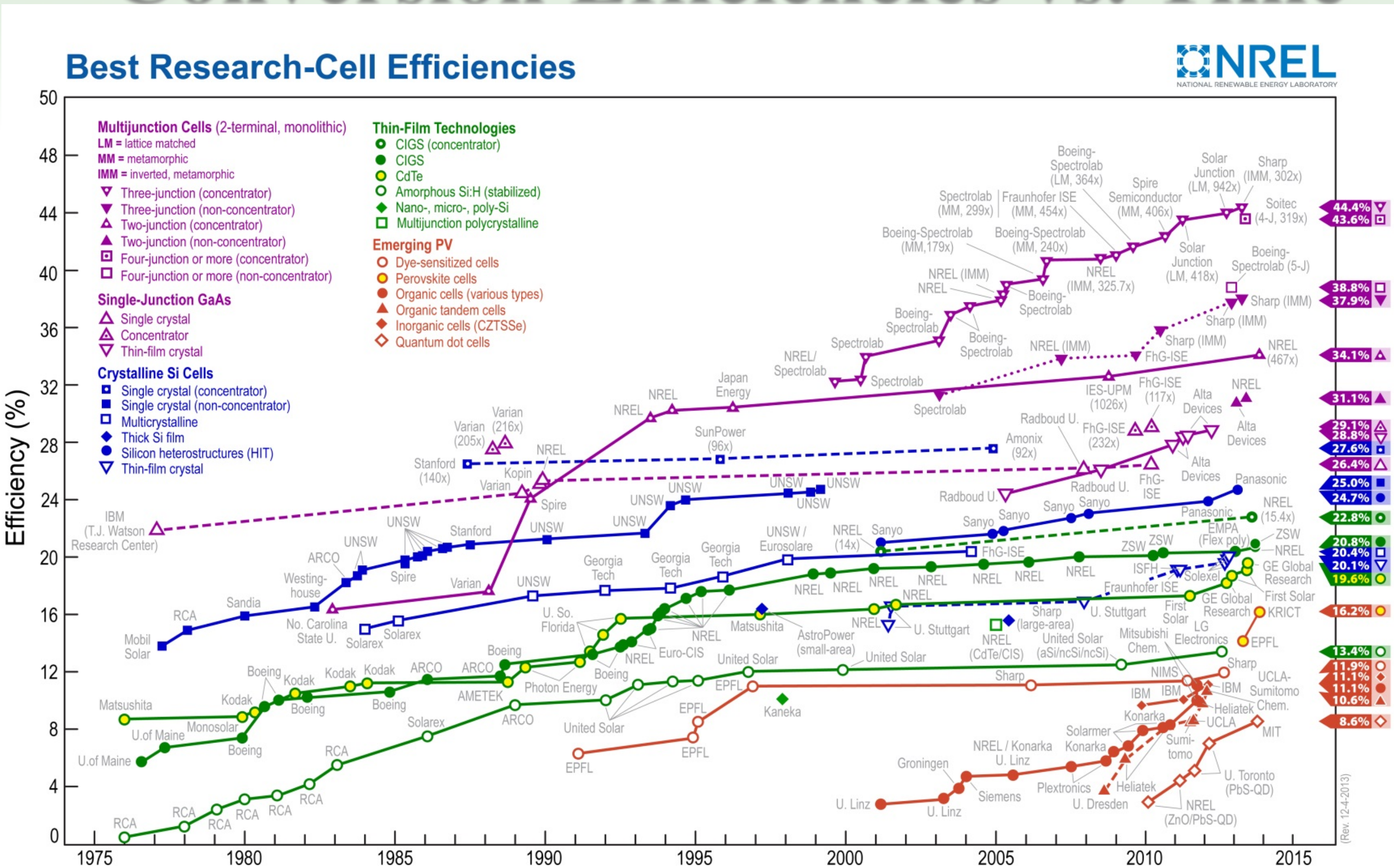

- There has been steady progress in the improvement of conversion efficiencies for a number of PV technologies over the last few decades.

The Typical Silicon Solar Cell

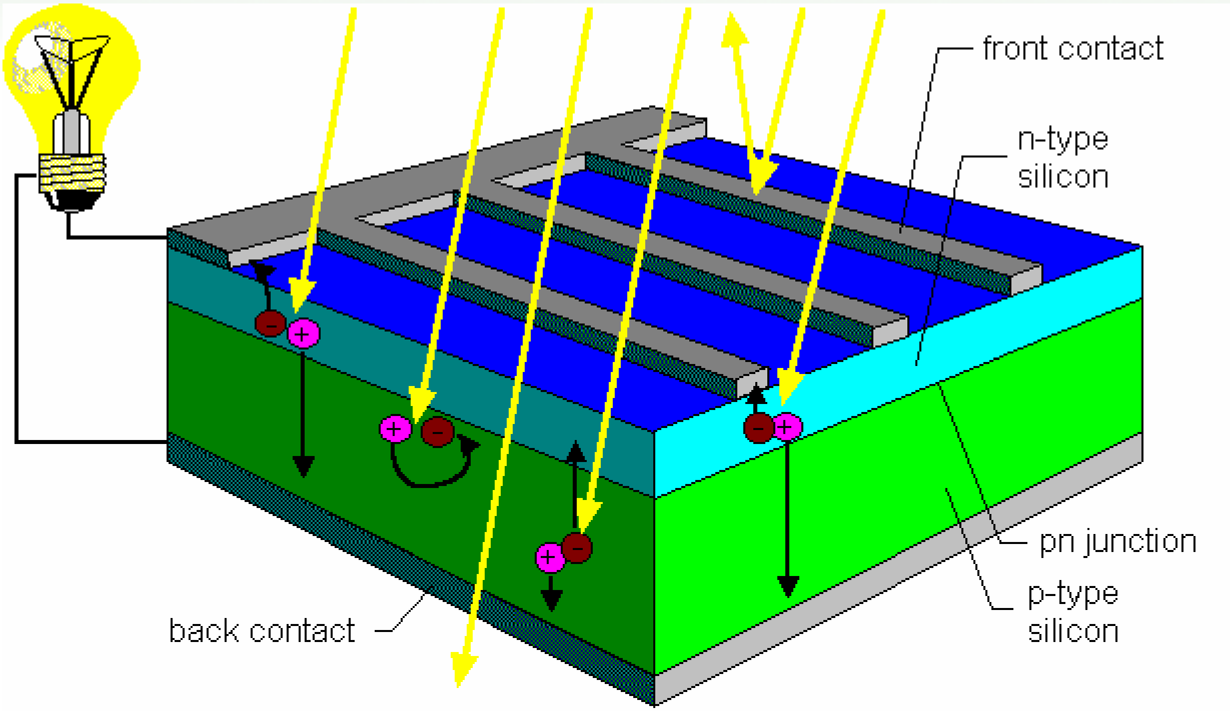

- **This device structure is used by most manufacturers today.**
  - **One piece of silicon has a small amount of boron added to it, which gives it a tendency to attract electrons. It is called the p-layer because of its positive tendency.**
  - **The other piece of silicon has a small amount of phosphorous added to it, giving it an excess of free electrons. This is called the n-layer because it has a tendency to give up negatively charged electrons.**
- **The cell efficiencies for screen-printed multicrystalline silicon cells are typically in the range of 14 – 17%.**

Copper-Indium-Gallium-Diselenide Cell

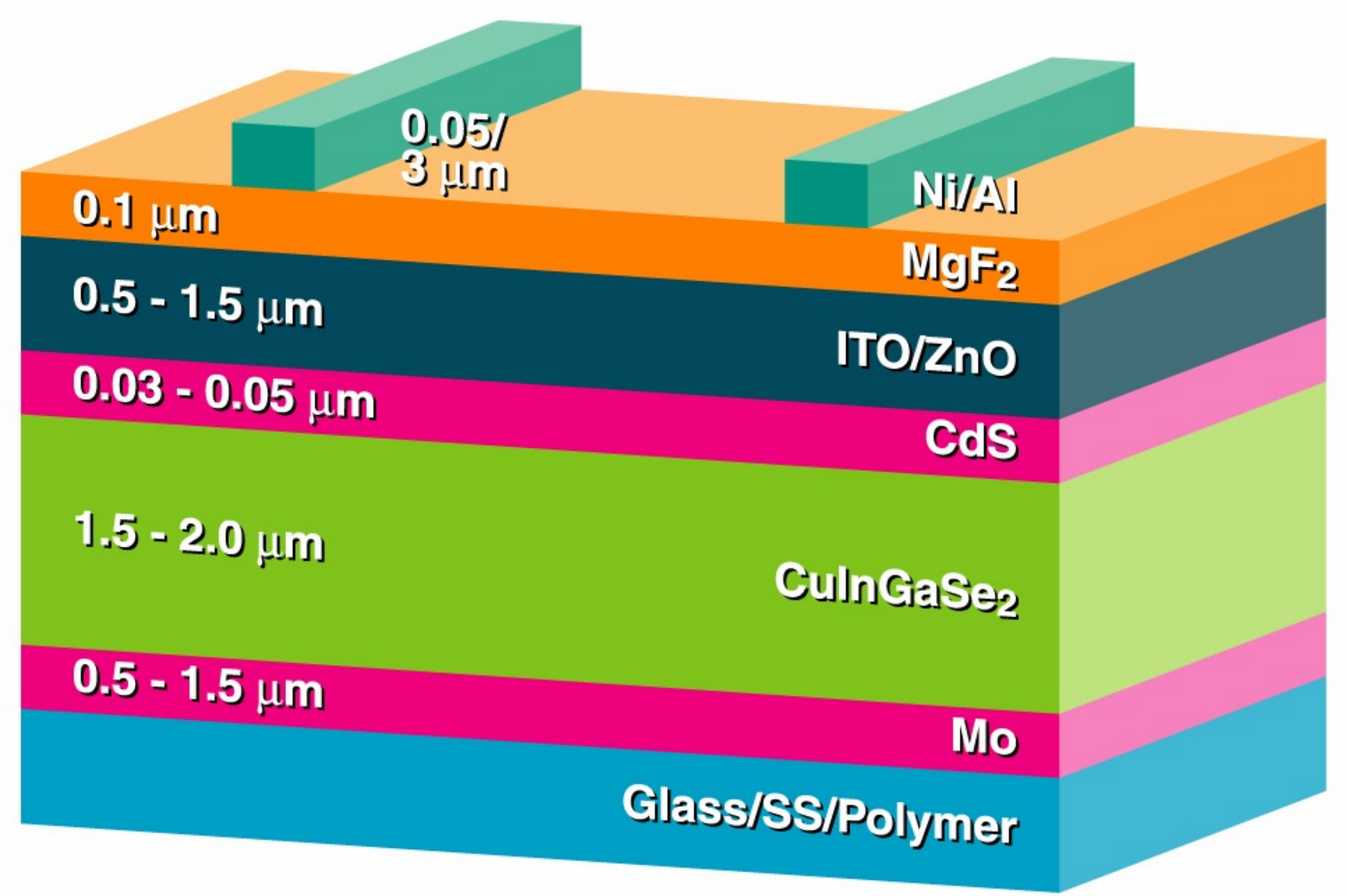

- EMPA has demonstrated an efficiency of 20.4% for the CIGS solar cell.
- It typically requires relatively high temperature processing (> 500°C).

Spectrolab's Triple-Junction Solar Cell

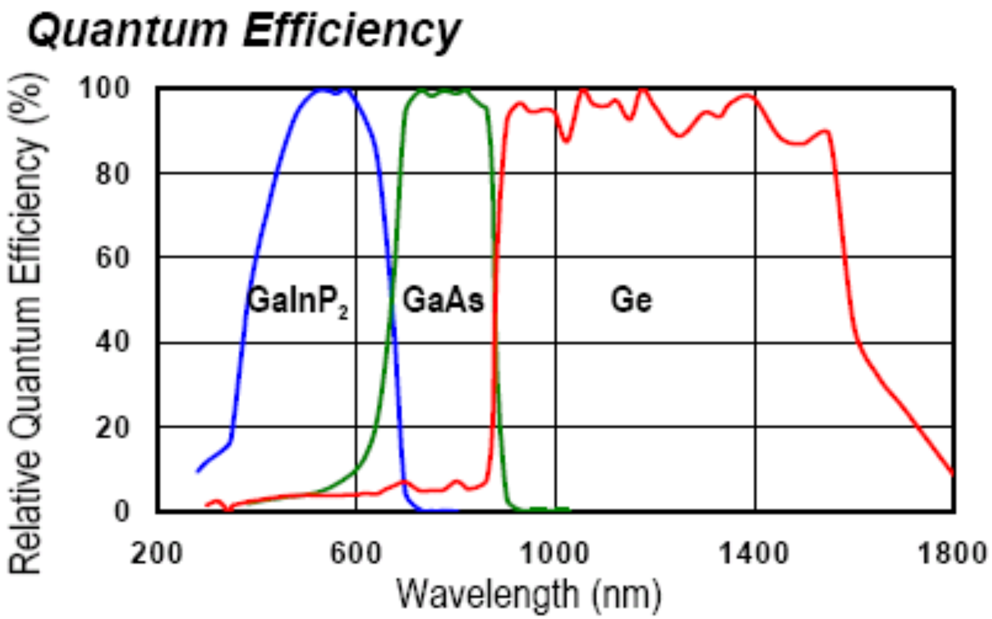

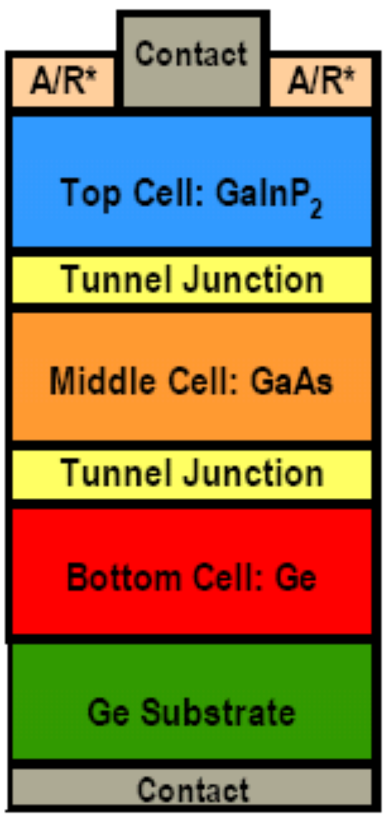

- Spectrolab has reported a conversion efficiency of 44.4% with this solar cell structure operating at Sharp.

The mechanism of power generation
Dye-sensitized solar cells

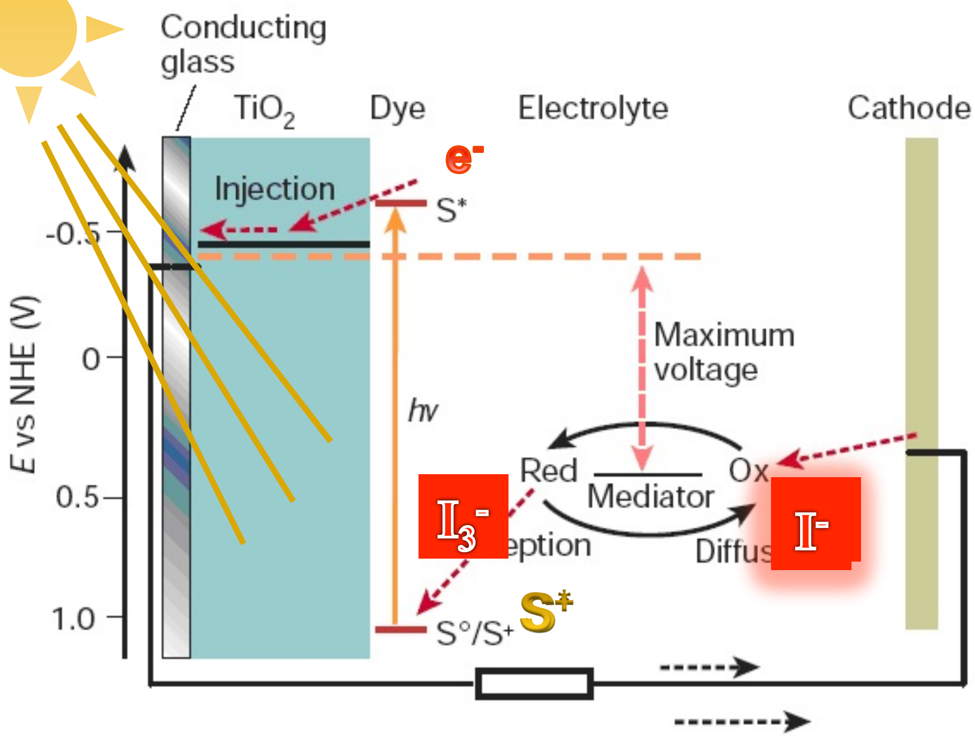

$$S + hv \rightarrow S*$$

$$S^* \rightarrow S^+ + e^- \rightarrow CB(TiO_2)$$

$$I_3^- + 2e^- \; CB(TiO_2) \rightarrow 3I^-$$

$$2S^+ + 3I^- \rightarrow 2S + I_3^-$$

$I_3^- + 2e^- \rightarrow 3I^-$

$S^+ + e^- \rightarrow S$

Basic Components and Parameter

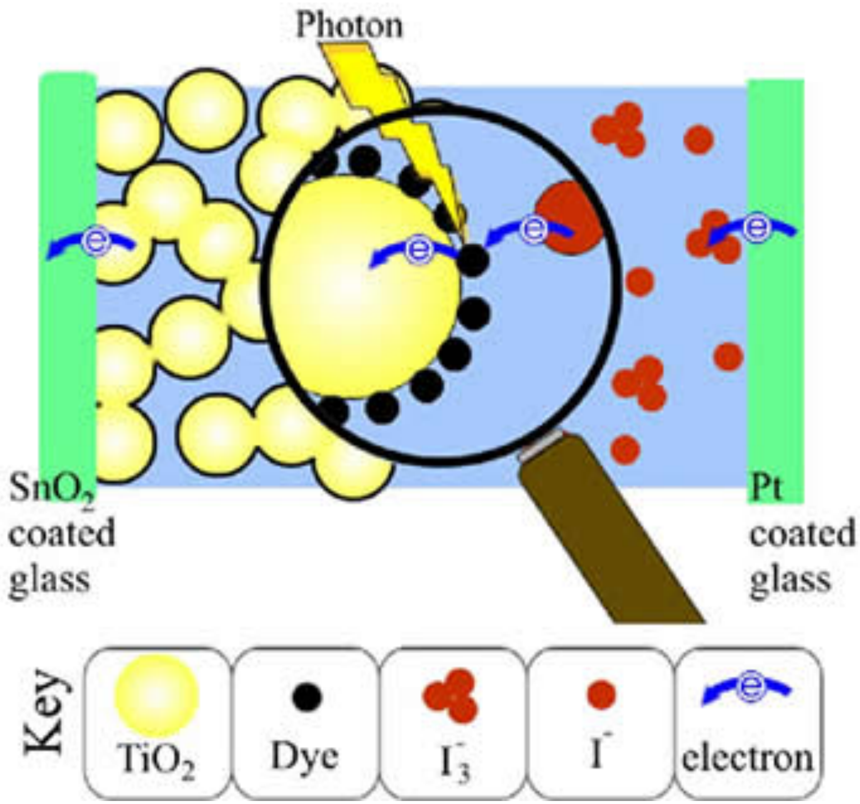

$$\eta = \frac{J_{sc} \bullet V_{oc} \bullet FF}{P_{in}}$$

$$IPCE(\lambda) = \frac{1240 \bullet J_{sc}}{\lambda \bullet P}$$

- ***J*sc-short-circuit photocurrent**
- ***V*oc-open-circuit photovoltage**
- **FF-fill factor**
- **IPCE-incident monochromatic photon-to-electron conversion efficiency**
- **η_{global}-The maximum energy conversion efficiency**

DSSCs

IPCE

By the product of
light harvesting efficiency (LHE),
electron injection efficiency(CIE),
and charge collection efficiency (CCE).

Jsc

Depends on IPCE

Voc

Derived from the difference between
the Fermi level of the TiO_2 electrode
and I^-/I_3^- redox potential

FF

The ratio of maximum obtainable power
to the product of the *Voc* and *Jsc*

Contents

Innovative Design

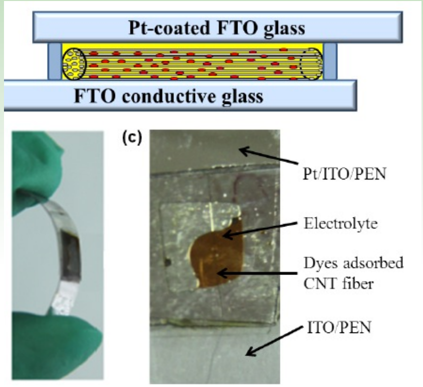

Carbon Nanotube Fiber

We first made a family of novel organic solar cells with excellent performance from the highly aligned nanotube fiber.

- **Excellent electrical properties**
- **Excellent mechanical properties**
- **Flexible Tunable diameters**

※ **Ref:** S. Wang, et.al *Angew. Chem., Int. Ed.*, 2011, **50**, 1855.

Carbon Nanotube Fiber

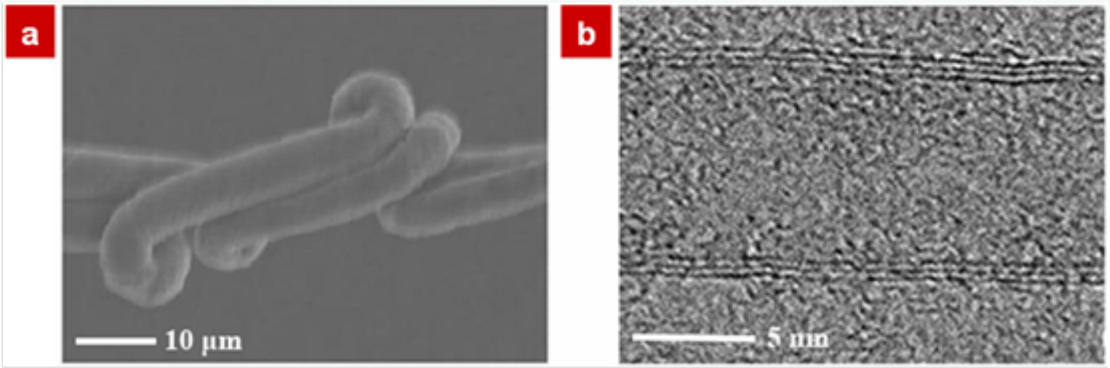

SEM and TEM

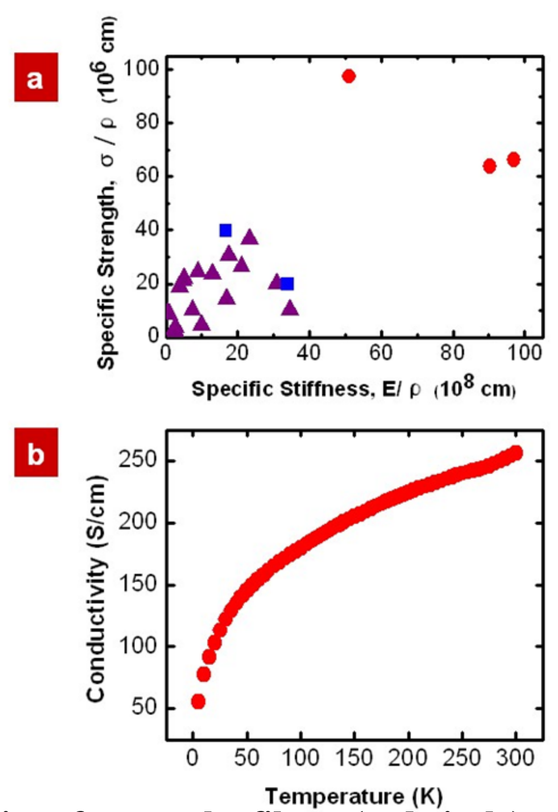

- The tying knots revealing the high flexibility and resistance to torsion of the nanotube fiber.
- The specific strength is 2.9 times of *T1000*, and the specific stiffness is 3.9 times of *M70J*.
- The conductivities increase with increasing temperatures.

a, Mechanical properties of nanotube fibers (red circle), engineering fibers (cyan triangle) and carbon fibers (blue square). b, Temperature dependence of the conductivity for a nanotube fiber.

Polydiacetylene -Well distributed

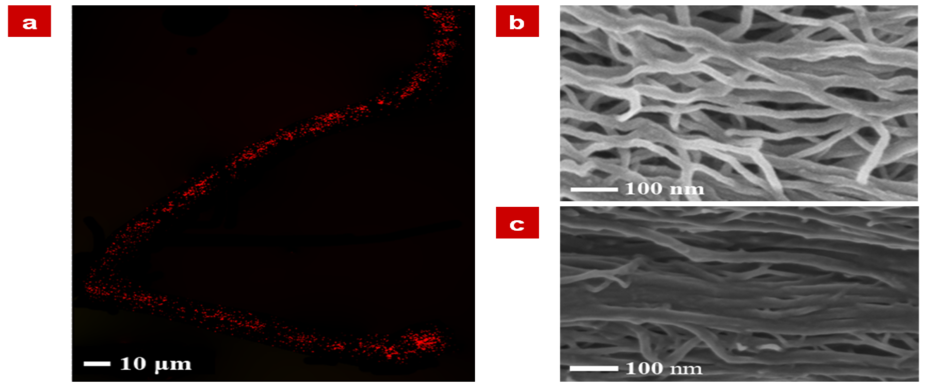

N719 molecules - also well distributed

a.) Confocal laser scanning microscopy image b,c) SEM images of a nanotube fiber before (b) and after (c) incorporation of N719.

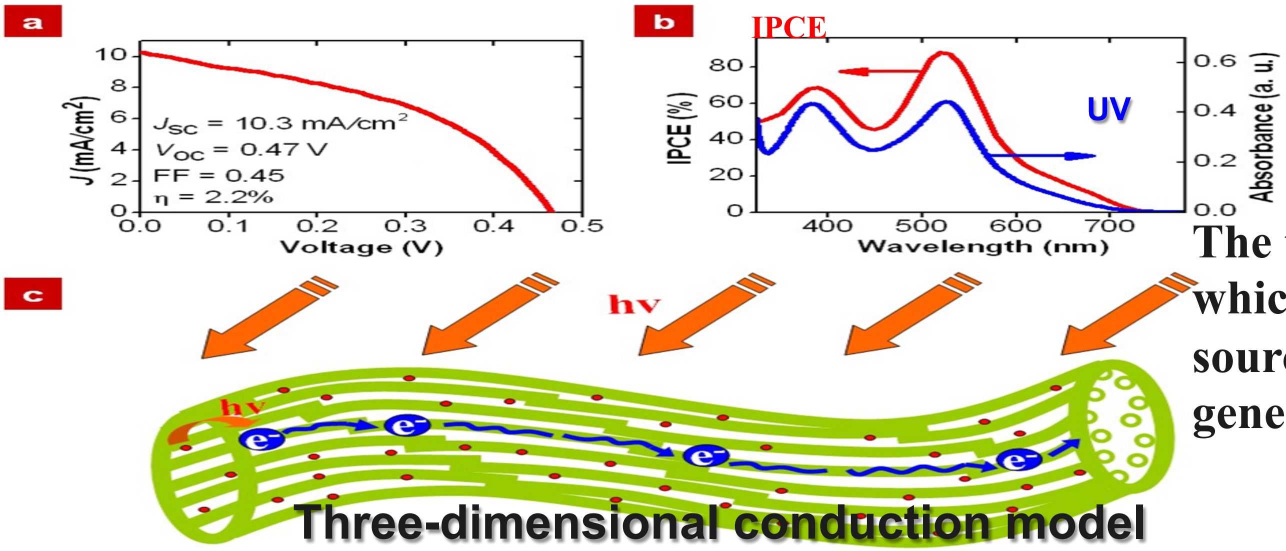

The two spectra are very similar, which indicates that N719 is the source of photocurrent generation.

a, J-V curve.
b, IPCE action spectrum (red line) and the UV-vis absorption spectrum of N719 in ethanol (blue line)
c, Schematic diagram

The nanotube fibers with different diameters

Diameter (μm)	Jsc (mA/cm^2)	Voc (V)	FF	η (%)
6	11.0±0.7	0.45±0.02	0.41±0.03	2.03±0.20
10	7.6±0.2	0.48±0.03	0.39±0.01	1.42±0.10
13	3.1±0.3	0.25±0.04	0.40±0.02	0.31±0.03
17	2.1±0.1	0.18±0.01	0.38±0.02	0.14±0.02

Current densities decreased with increasing fiber diameters

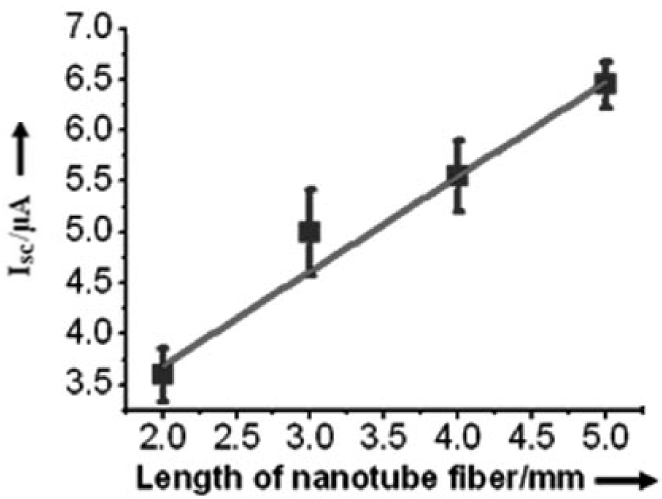

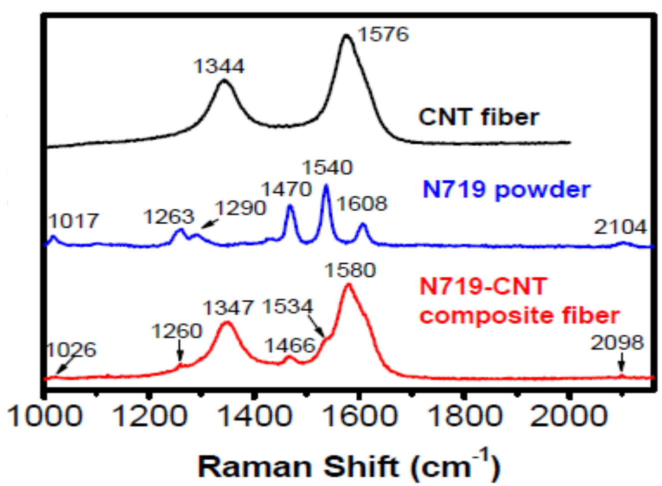

Through π-π interactions and van der Waals forces

Dependence of the shortcircuit current on the length (left), Raman spectra (right)

Conclusions

- High alignment of building nanotubes allows charges to separate and transport along the fibers efficiently.
- Expands the scope of materials and architectures available for high-performance photovoltaic devices.

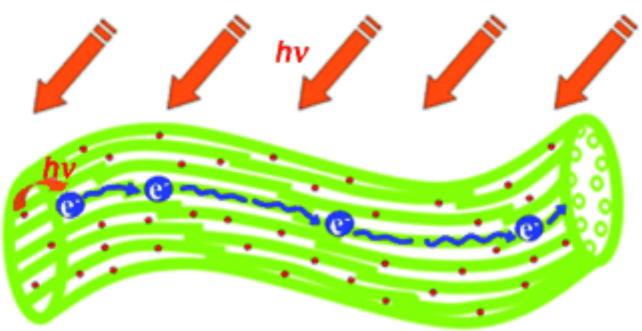

Contents

Titanium dioxide

Rutile

Anatase

Brookite

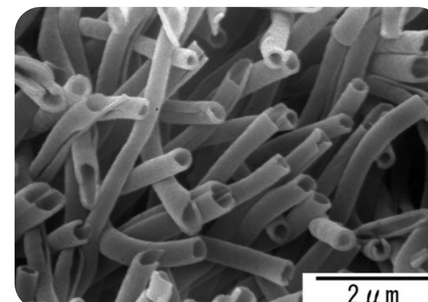

Nanotubes

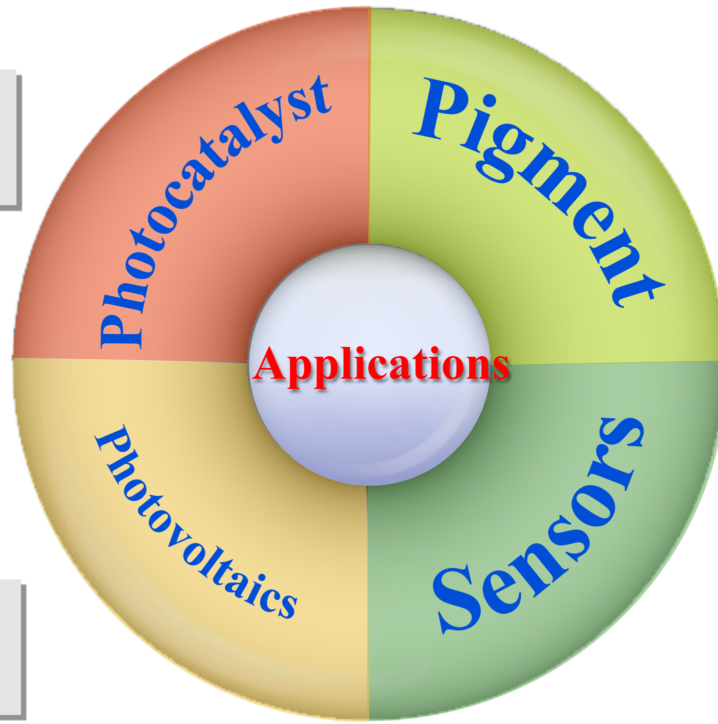

Nanoparticle-TiO_2

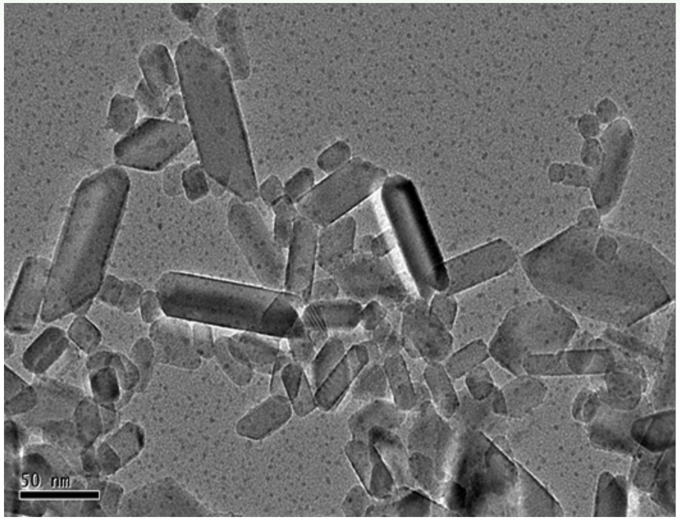

20:1

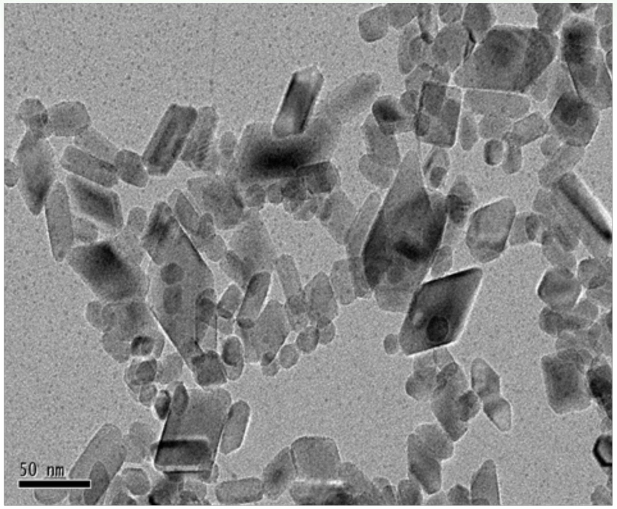

40:1

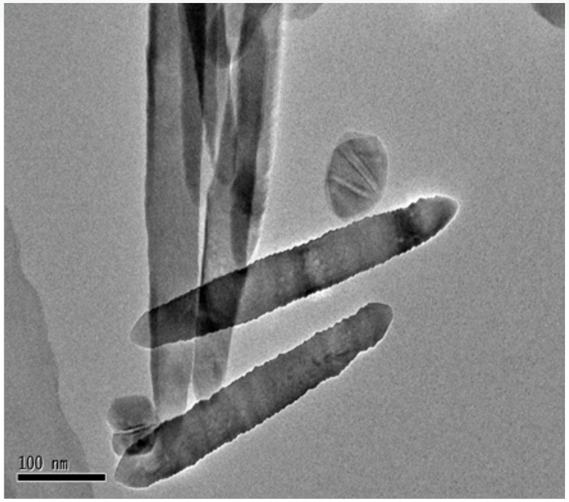

4% Zn doped of 20:1

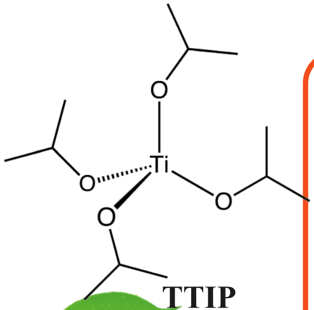

- TTIP
- deionized water

25℃ 1h

hydrolysis

120℃ 4h

- precipitate
- TMAH

hydrothermal process

- autoclave
- mixture

220℃ 12h

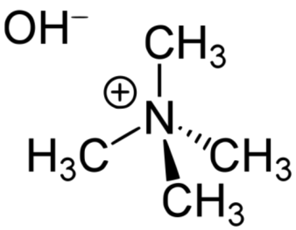

Doping one- Zn/W Doping on FF

Previous Studies

Thesis Research

η is determined by the product of *Voc*, *Jsc*, and FF

The analysis on FF is relatively rare

Zn-doped and W-doped DSSCs study on FF

Doping one- Zn/W Doping on FF

Table. Measured performance parameters of all the DSSCs

DSSC series	Doping amount	J_{sc} (mA cm^{-2})	V_{oc} (mV)	*FF* (%)	η (%)	*R* at V_{oc}/Ω	*m*
Zn-doped	0%	7.63 ± 0.03	754 ± 3	72.4 ± 0.1	4.17 ± 0.03	37.0 ± 1.0	2.47 ± 0.02
	0.5%	8.15 ± 0.02	799 ± 3	75.4 ± 0.2	4.91 ± 0.02	35.2 ± 0.4	2.20 ± 0.01
	1.0%	7.86 ± 0.01	785 ± 3	76.4 ± 0.0	4.71 ± 0.01	34.2 ± 0.2	2.07 ± 0.02
	2.0%	7.69 ± 0.00	777 ± 3	77.6 ± 0.1	4.64 ± 0.01	36.9 ± 0.2	1.86 ± 0.02
	3.0%	6.42 ± 0.02	787 ± 3	77.8 ± 0.3	3.94 ± 0.01	37.3 ± 0.6	1.85 ± 0.01
	4.0%	7.52 ± 0.03	811 ± 3	78.3 ± 0.1	4.77 ± 0.03	32.5 ± 0.5	1.86 ± 0.02
	10.0%	6.95 ± 0.01	831 ± 3	78.6 ± 0.1	4.54 ± 0.00	35.3 ± 0.2	1.89 ± 0.02
W-doped	0%	7.03 ± 0.01	620 ± 1	77.0 ± 0.2	3.36 ± 0.02	26.3 ± 0.2	1.51 ± 0.01
	0.1%	7.43 ± 0.04	620 ± 1	76.8 ± 0.6	3.54 ± 0.02	24.9 ± 1.0	1.51 ± 0.01
	0.2%	8.99 ± 0.01	610 ± 1	76.4 ± 0.3	4.19 ± 0.03	21.2 ± 0.2	1.54 ± 0.01
	0.5%	9.06 ± 0.02	604 ± 1	69.6 ± 0.4	3.81 ± 0.01	24.8 ± 0.4	2.16 ± 0.01
	1.0%	9.20 ± 0.01	594 ± 1	69.0 ± 0.2	3.77 ± 0.00	26.6 ± 0.2	2.21 ± 0.00
	2.0%	9.54 ± 0.02	592 ± 1	67.0 ± 0.1	3.78 ± 0.02	25.9 ± 0.4	2.59 ± 0.01

m can reflect the leakage of current and carrier and non-radiative recombination caused by defects, can characterize the device reliability.

$$V_{oc} = V_m + \frac{mkT}{q}\cdot\ln\left(1+\frac{qV_m}{mkT}\right)$$

$$FF = \frac{J_m V_m}{J_{sc} V_{oc}} = \frac{\frac{qV_m^2}{mkT}\cdot\exp\left(\frac{qV_m}{mkT}\right)}{V_{oc}\left[\exp\left(\frac{qV_{oc}}{mkT}\right)-1\right]}$$

$$m = \frac{q}{KT}\bullet\frac{dV}{d(\ln I)}$$

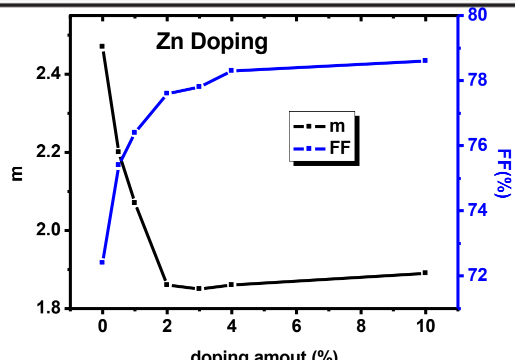

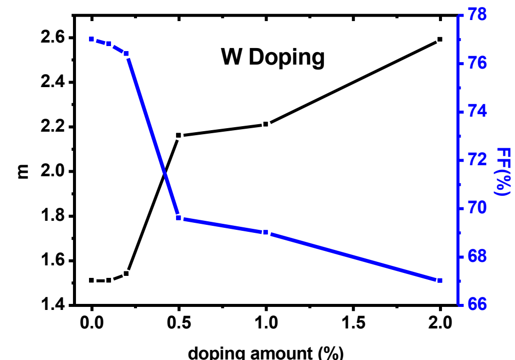

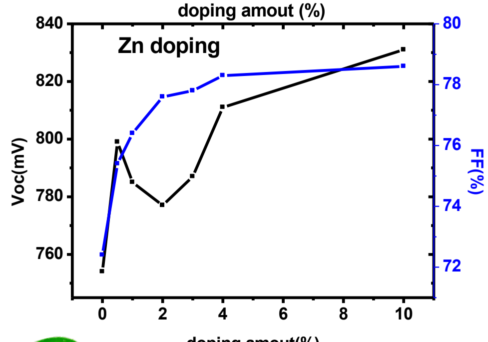

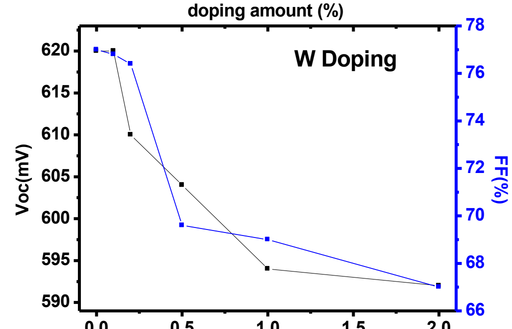

※ **Ref:** S. Wang, et.al, *Appl. Phys. Lett.*, 2011, **99**, 113503.

Doping one- Zn/W Doping on FF

◆ Zn:

- The increase in FF with doping amount is due to doping induced improvement of *Voc* and reduction of m

◆ W:

- W-doping induced increase in m and decrease in *Voc* result in the reduction of FF

◆ Conclusion:

- The ratio of *Voc*/m could directly determine FF in a high-accurate approximation for the cells

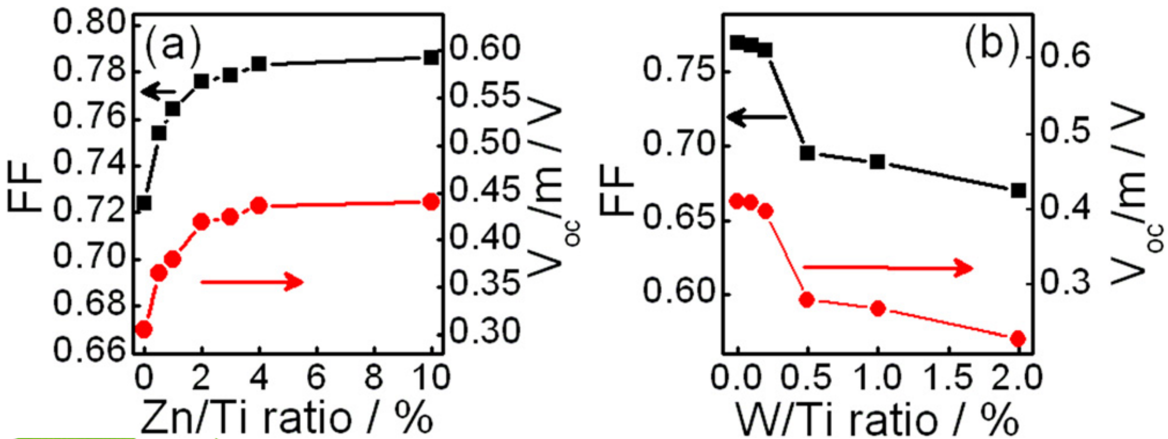

Dependences of FF and the ratio Voc/m on doping amount

Shed light on the influencing factors of FF and guide the design of new materials towards high FF for DSSCs

※ **Ref:** S. Wang, et.al, *Appl. Phys. Lett.*, 2011, **99**, 113503.

Doping two- Fe^{2+}/Fe^{3+} Doping

As compared to the typical single valence state of metal ions (Fe^{3+})-doped DSSCs, the multi-valence -doped DSSCs improves short-circuit photocurrent (J_{sc}) by 17.6% and power conversion efficiency by 17.2%.

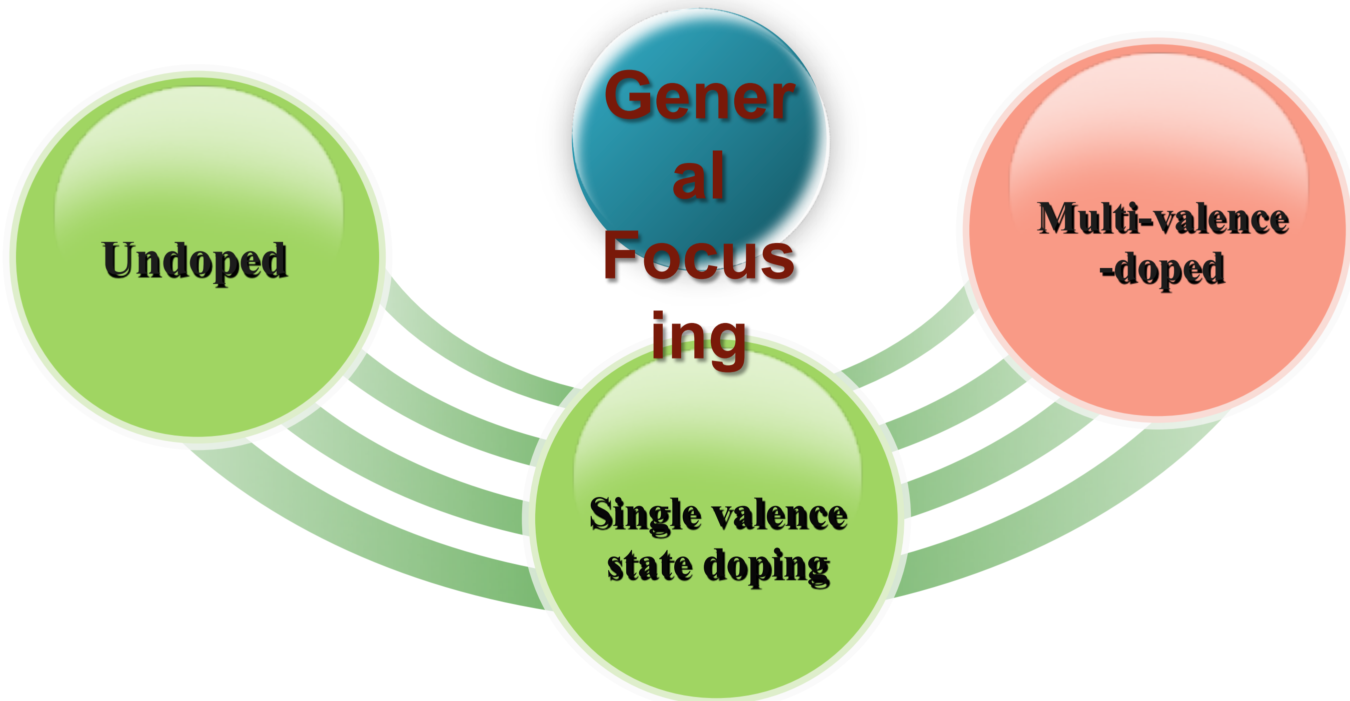

Doping two- Fe^{2+}/Fe^{3+} Doping

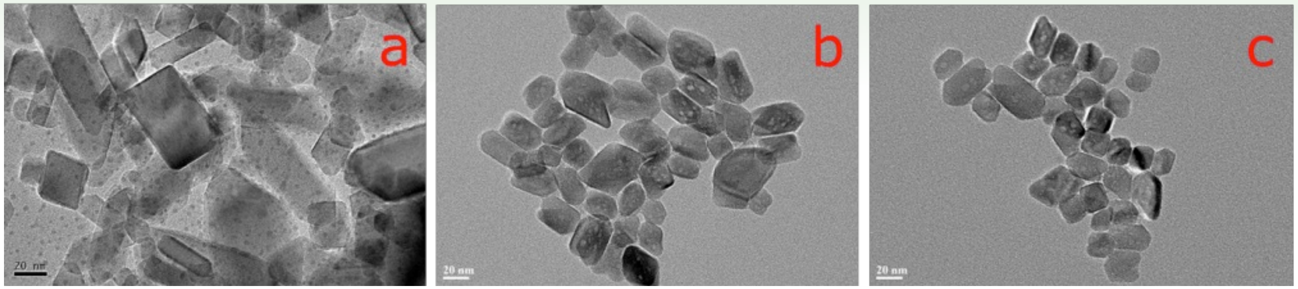

The surface of Fe^{2+}-doped TiO_2 particles become steric regularity and homogeneously.

TEM of (a) undoped, (b) 0.5wt% Fe^{2+} doped and (c) 1wt% Fe^{2+} doped

◆ Shifted toward the higher energy side
◆ 532.0 eV implies surface OH^- groups or chemisorbed water molecules
◆ Fe^{2+}-Fe^{3+} co-exist for 0.5wt% Fe^{2+} ions doping

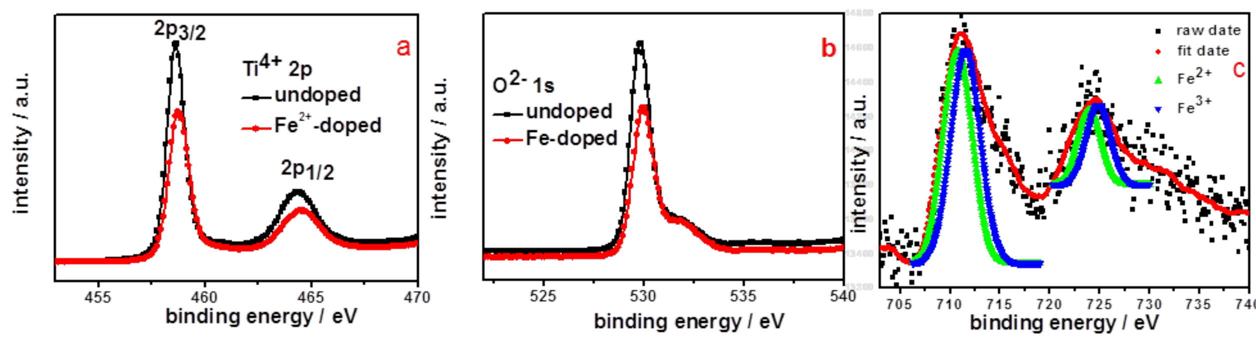

XPS spectra: (a), Ti^{4+} 2p (b), O^{2-} 1s (c), and Fe 2p

※ **Ref:** S. Wang, et.al, **2012** , CN102751099A, Chinese patent

Doping two- Fe^{2+}/Fe^{3+} Doping

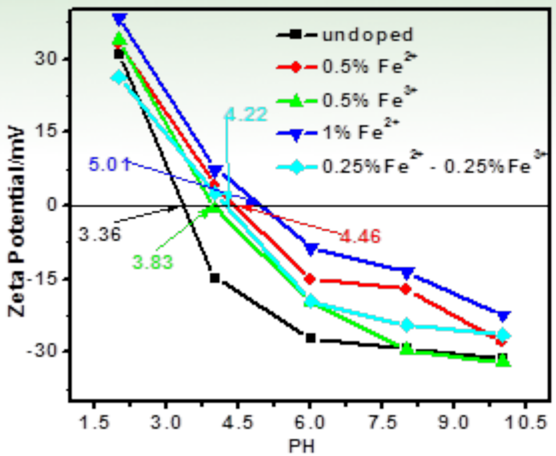

Isoelectric points

Positive surface

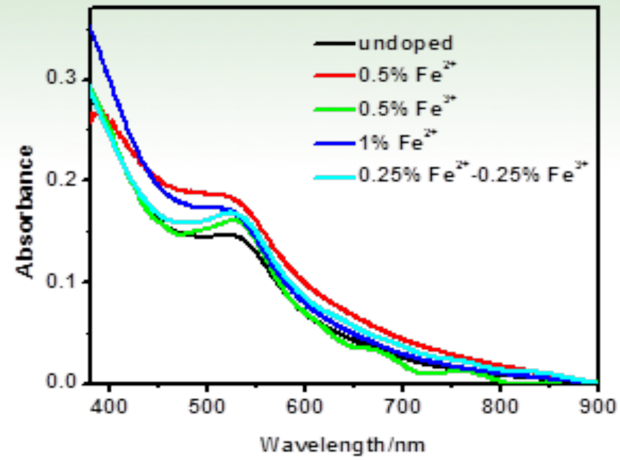

Absorbance spectra of the absorbed dye on the samples

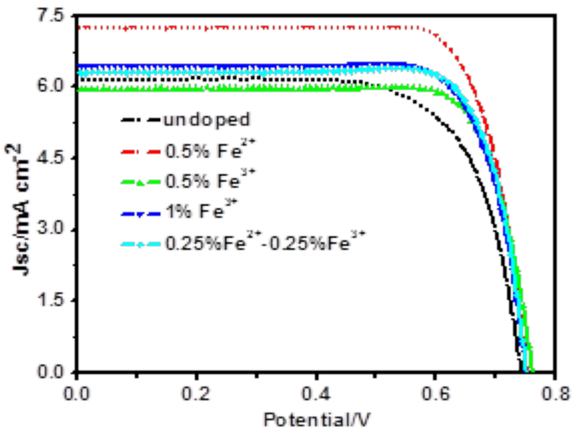

Current–voltage curves of DSSCs

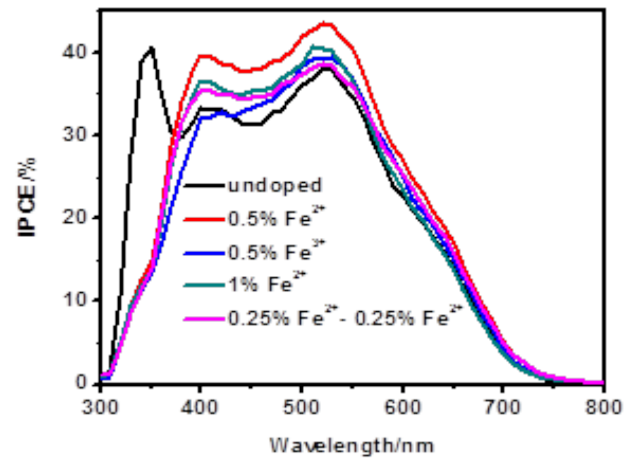

IPCE spectra of DSSCs

※ **Ref:** S. Wang, et.al, **2012** , CN102751099A, Chinese patent

Conclusions

- The dependence of FF on *Voc* and m for DSSCs with Zn- or W-doped TiO_2 is analyzed based on a single-diode model.

- Fe-doping results in a relatively positive surface, and reduces the direct excitation of TiO_2.

Contents

Innovative Design

$SrCO_3$ layer suppress charge recombination and a fresh TiO_2 layer available for efficient electron injection

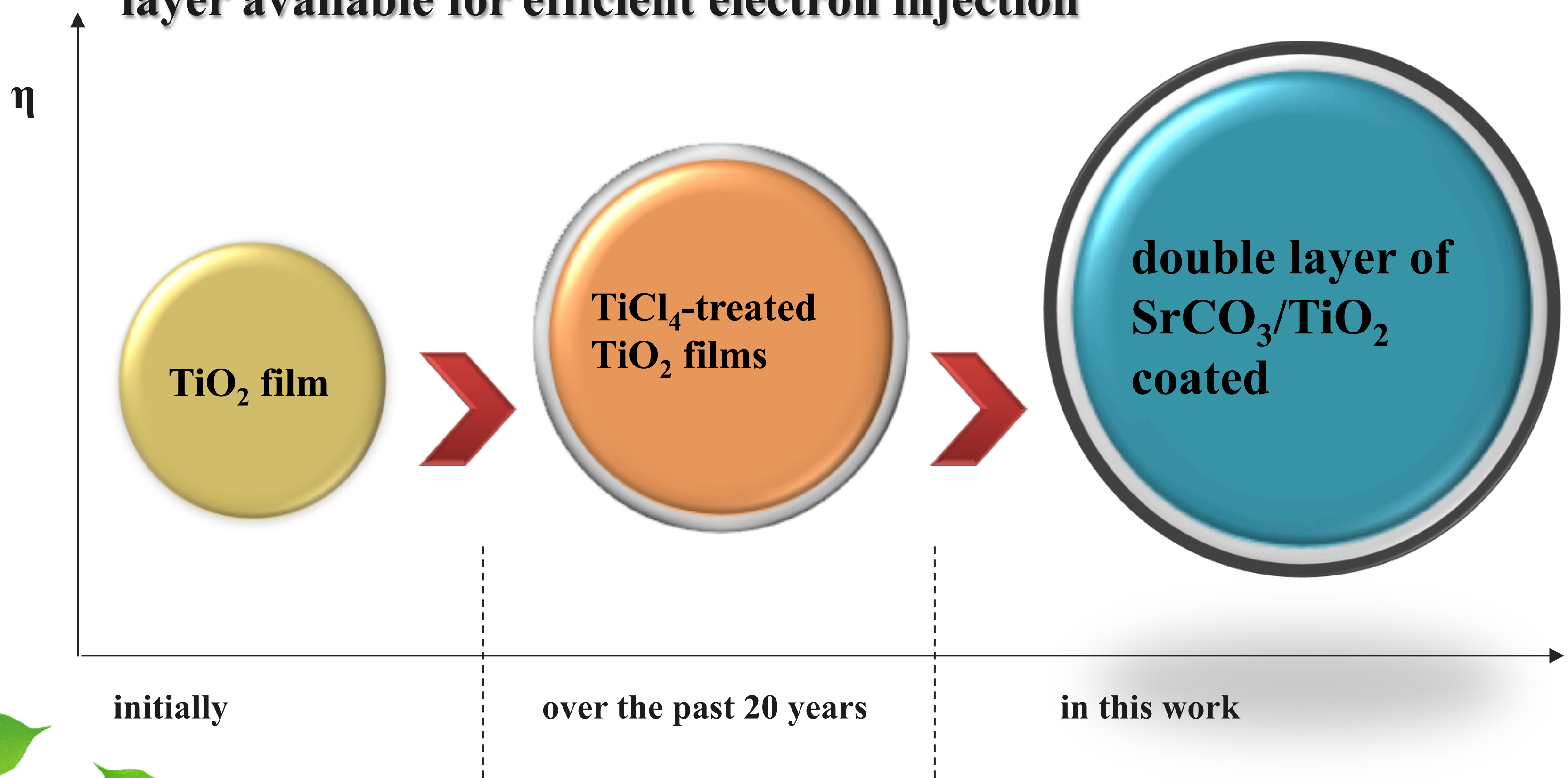

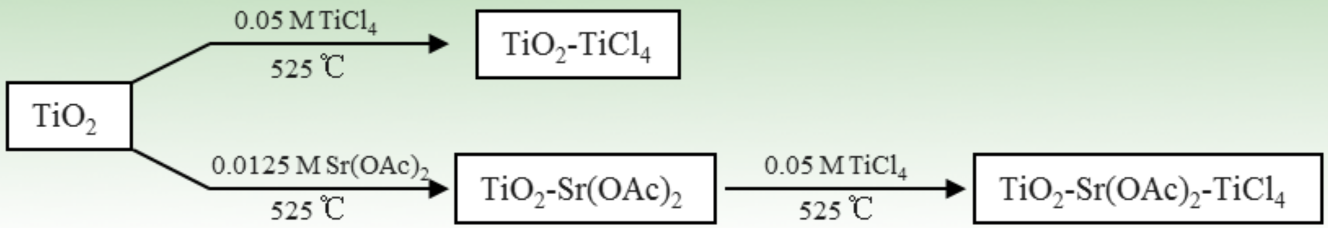

Procedures for surface treatments

TGA curve

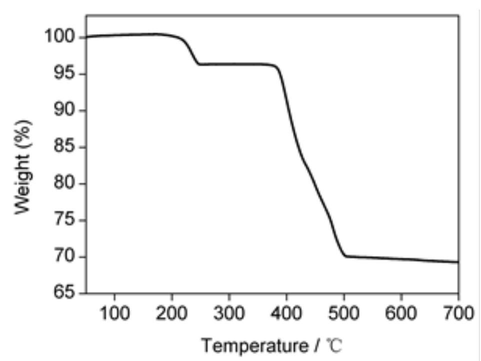

FTIR spectra

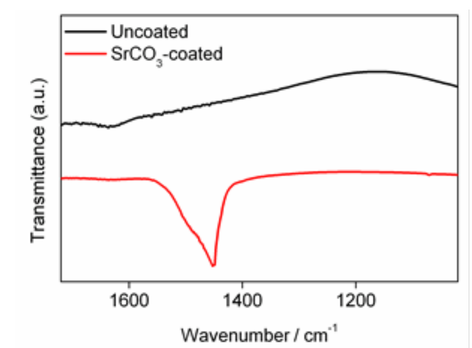

$$Sr(CH_3COO)_2 \bullet \frac{1}{2}H_2O \xrightarrow{-\frac{1}{2}H_2O} Sr(CH_3COO)_2 \xrightarrow{+4O_2} SrCO_3(s) + 3H_2O(g) + 3CO_2(g)$$

※ **Ref:** S. Wang, et.al, *Phys. Chem. Chem. Phys.*, 2012, **14**, 816.

	Sr/Ti ratio	J_{sc} / mA cm^{-2}	V_{oc} / V	FF	η (%)
TiO_2		6.28±0.06	0.788±0.012	0.69±0.02	3.41±0.12
TiO_2-$TiCl_4$		7.53±0.07	0.815±0.015	0.69±0.01	4.23±0.04
TiO_2-$Sr(OAc)_2$-$TiCl_4$	0.02%	8.83±0.06	0.833±0.005	0.69±0.01	5.08±0.03

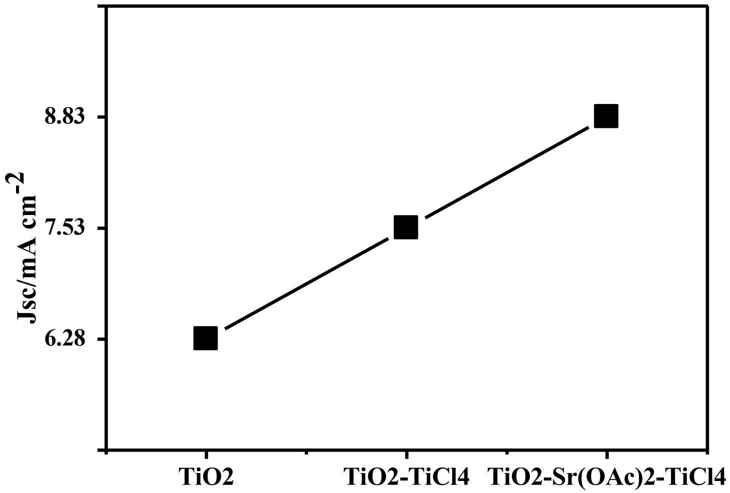

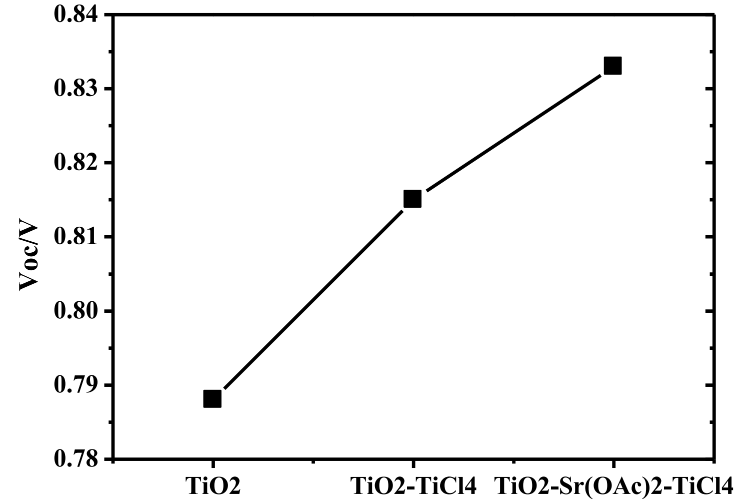

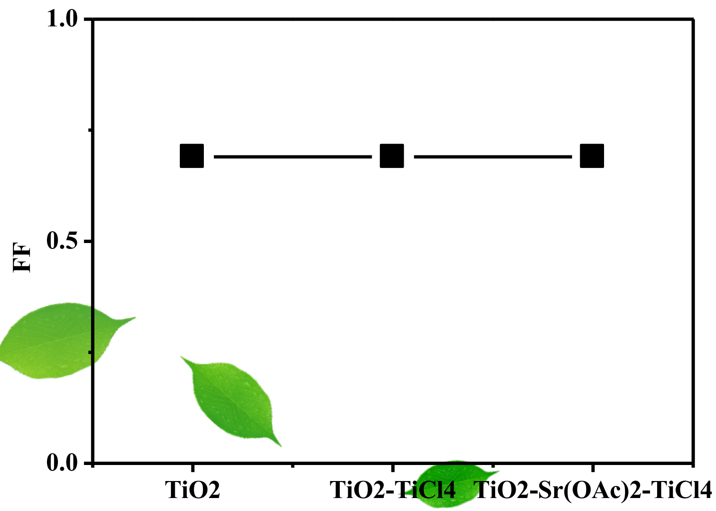

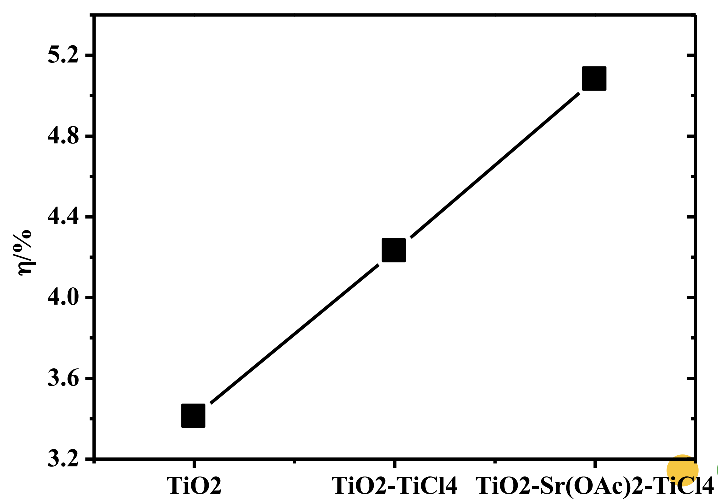

Double Layer Coating

Compared $TiCl_4$-treated

Compared untreated TiO_2

Improved *Jsc* by 17%, *Voc* by 18 mV, and *η* by 20%

We fabricated thin films(4.49 ± 0.05 μm) through one-printing

Improved *Jsc* by 41%, *Voc* by 45 mV, and *η* by 49%

Effect on dye adsorption and IPCE

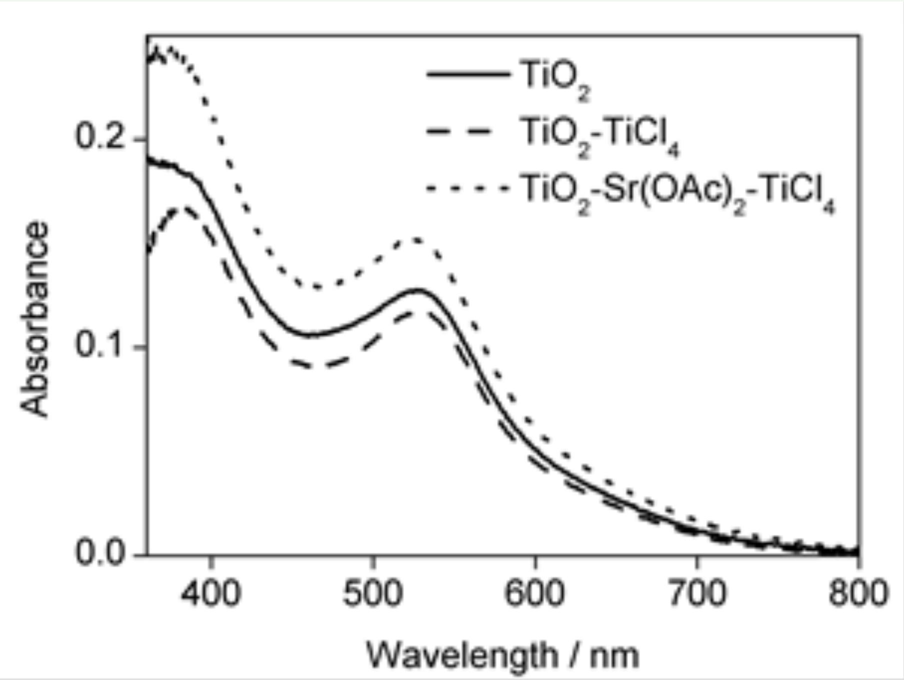

UV-vis spectra for the N719-loaded films

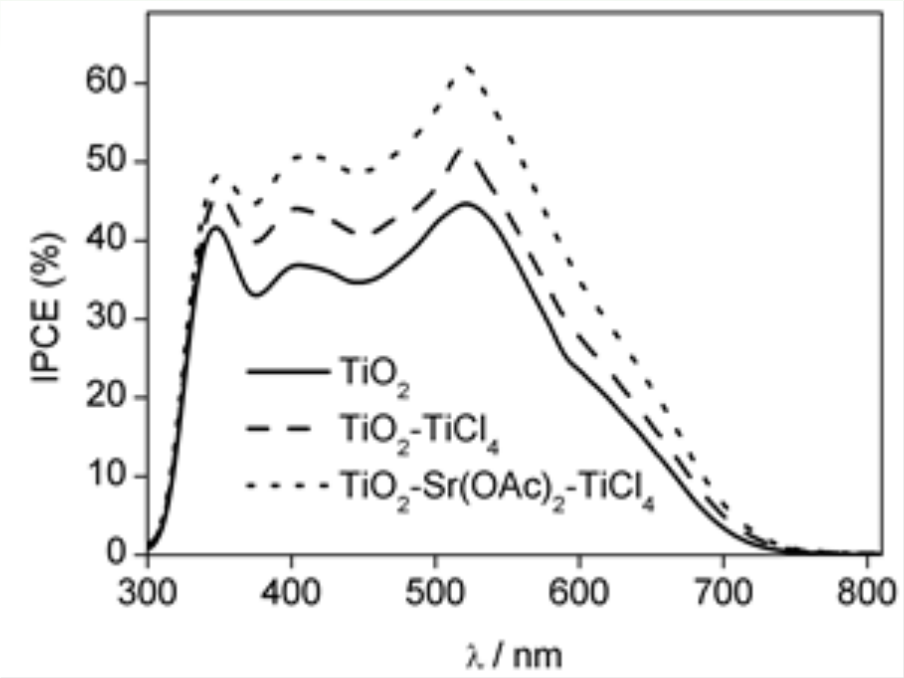

IPCE spectra

The $Sr(OAc)_2$–$TiCl_4$ treatment enhanced dye loading is attributed to the higher isoelectric point for $SrCO_3$ than that for TiO_2

CIE and CCE both must also be responsible for the significant increase in IPCE.

※ **Ref:** S. Wang, et.al, *Phys. Chem. Chem. Phys.*, 2012, **14**, 816.

Effect on conduction band level and electron transport

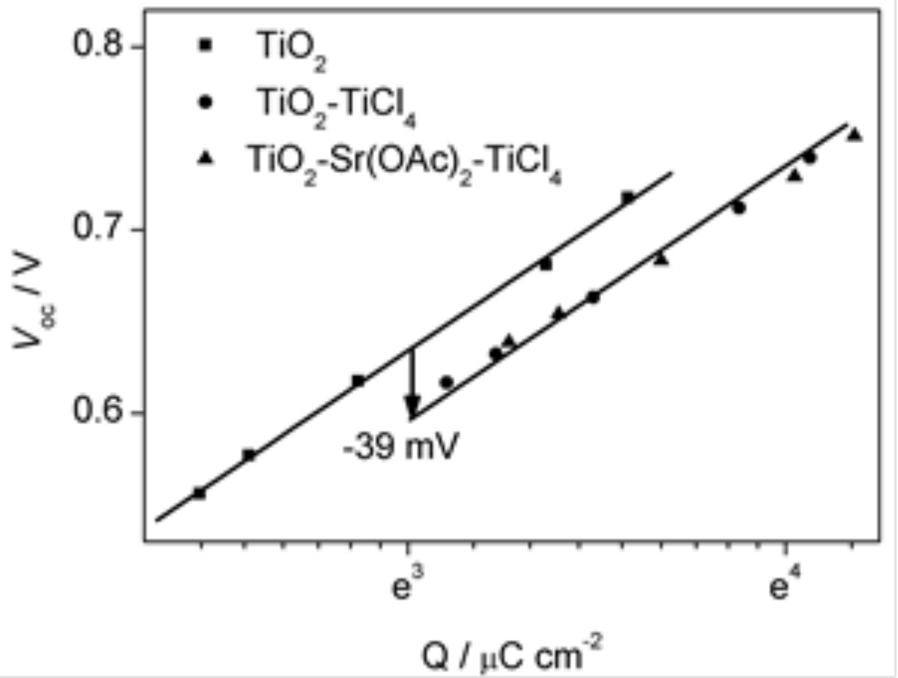

Open-circuit photovoltage as a function of charge density at open circuit

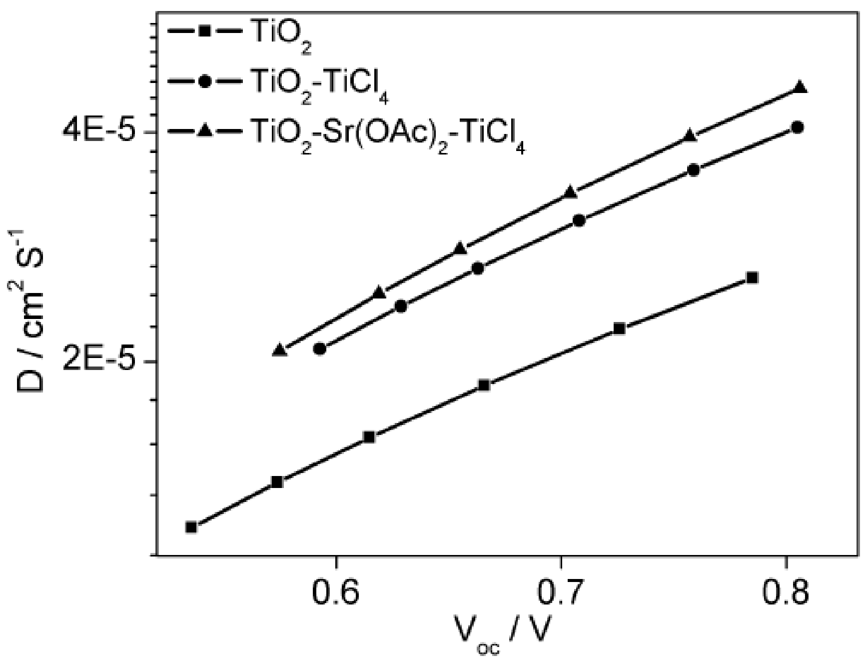

electron diffusion coefficient

The surface charge of the TiO_2–$Sr(OAc)_2$–$TiCl_4$ electrode is dominantly controlled by the final-step of $TiCl_4$ treatment

Trap density is reduced by $TiCl_4$ treatment and further reduced by $Sr(OAc)_2$–$TiCl_4$ treatment.

※ **Ref:** S. Wang, et.al, *Phys. Chem. Chem. Phys.*, 2012, **14**, 816.

Effect on charge recombination

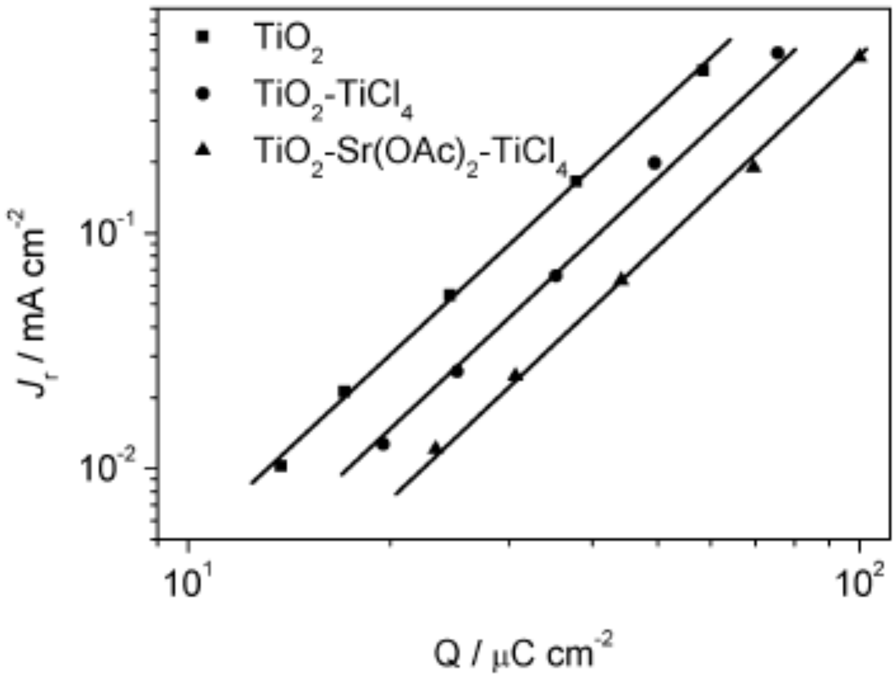

recombination current vs. charge density

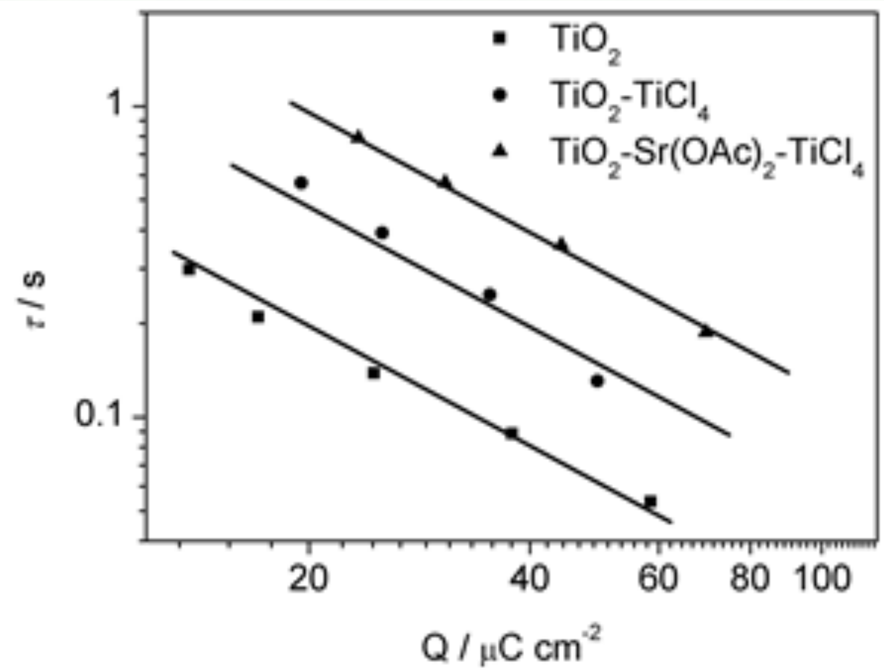

electron lifetime against charge density

The introduced electronically insulating layer of $SrCO_3$ layer further decreases the recombination rate constant by 2-fold

Treatment with $Sr(OAc)_2$ followed by $TiCl_4$ treatment further improved the electron lifetime by 2-fold

※ **Ref:** S. Wang, et.al, *Phys. Chem. Chem. Phys.*, 2012, **14**, 816.

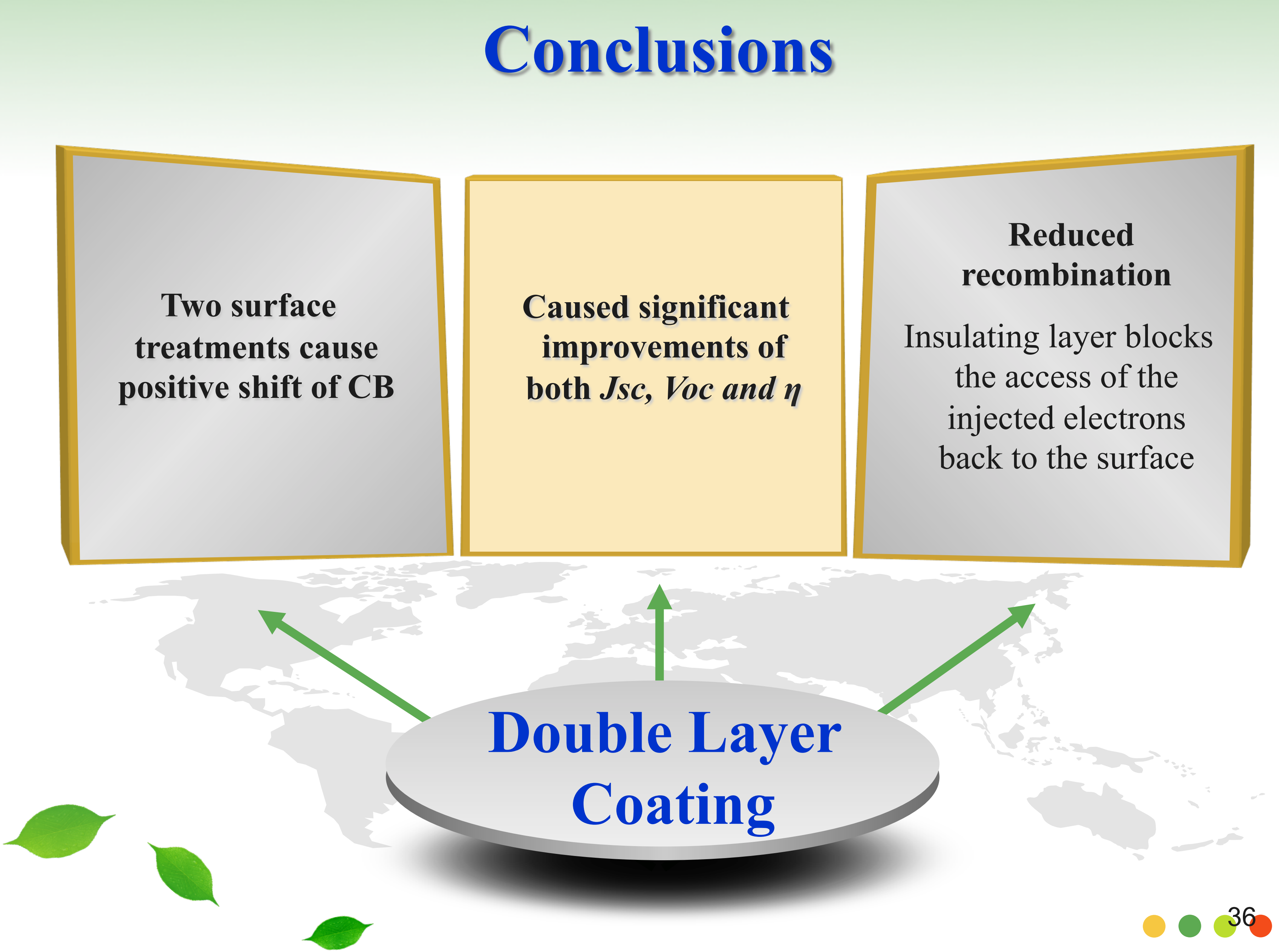

Conclusions
Two surface treatments cause positive shift of CB
Caused significant improvements of both Jsc, Voc and η
Reduced recombination
Insulating layer blocks the access of the injected electrons back to the surface
Double Layer Coating

Summary

Novel solar cell from flexible, light-weight, ultrastrong, and semiconductive nanotube fiber

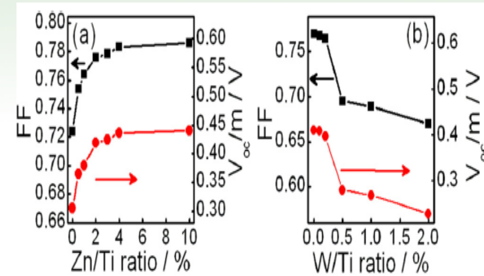

FF increases with the doping amount of Zn(II) but decreases with W(VI) in TiO_2

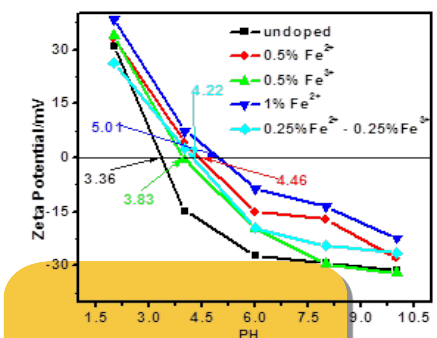

Modify surface polarity that caused surface positively charged, repressed charge recombination

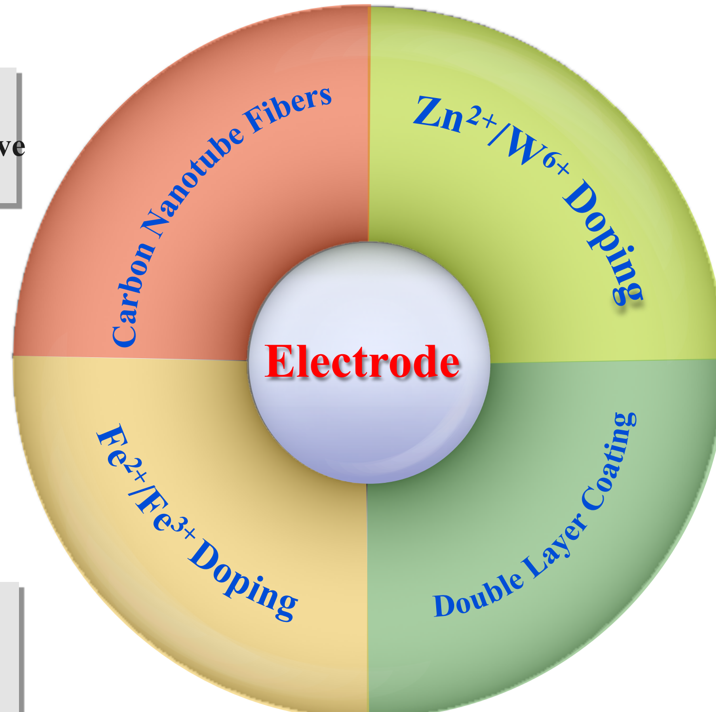

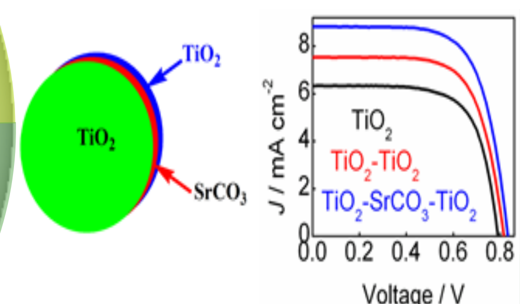

Insulating layer of $SrCO_3$ increases dye adsorption and improves charge separation efficiency

Thanks！